Harvesting energy from vehicle transportation on highways using piezoelectric and thermoelectric technologies

Harvesting energy from vehicle transportation on highways using piezoelectric and thermoelectric technologies

M A Mujaahiid Lallmamode and A S Mahdi Al-Obaidi

School of Computer Science and Engineering, Faulty of Innovation and Technology, Taylor's University, Selangor DE, Malaysia

E-mail: abdulkareem.mahdi@taylors.edu.my

Abstract. For many years, the rate of energy consumption has been higher than the rate at which natural resources are being generated. Green energy is a major solution to achieve a sustainable future and mitigate carbon footprints. Today, the transport sector highly relies on fossil fuel, consuming nearly one-quarter of the total energy in developed countries and represents a massive environmental burden. Hence, the fate of future energy security does not solely lie in the efficient use of existing green energies but also in the development of new energy sources. This study proposed the design of thermoelectric and piezoelectric energy harvesting systems to make use of the huge thermal energy due to solar radiation and mechanical strain due to moving vehicles to generate electricity. Both systems were built at an experimental scale model and tested. The thermoelectric system produced an output power of 1.06 mW and an open-circuit voltage of 118.2 mV at a temperature difference of 14.8 °C. A maximum average power output of 1.55 mW is achieved over a period of 6h per day. The Piezoelectric generated a peak DC voltage of 9.83 V, under normal stress of 235.04 kPa. The results also showed that the piezoelectric system could provide a consistent output voltage as long as the system experience normal stress. The system could produce an output power of 0.2 mW.

1. Introduction

Over the last decades, the disastrous impact of using non-renewable energy sources has threatened the world. Human health, global warming and pollutions are some of the main consequences caused by the use of limited non-renewable energies [1]. According to Malaysia energy statistics, the transport sector is the most significant energy-consuming sector, by using up to 42% of its energy demand [2]. Until now the transport sector highly relies on fossil fuel, which is over consumed and is expected to run out in a few decades [3]. In addition, solely 10% to 16% of the energy provided by fossil fuel is estimated to overcome resistance forces such as air drag and friction from the road [4]. Thus, the remaining energy is lost in mechanical vibration, heat, and strain [5]. The noticeable solar radiation absorbed by pavement surface is unutilized and very often leads to shortcomings such as the heat island effect in urban areas. Recuperating a portion of these local forms of energy as electricity would ameliorate the energy efficiency of road transportation and cities [6]. However, the fate of future energy security does not exclusively rely on the efficient use of

existing green energies but also the development of new energy sources [7]. Hence, the urgent need to move towards green energy and to collect the wasted energy on roads is more alarming than ever.

With the rapid advancement of technology, sustaining the power requirement for autonomous electronic systems, wireless sensors and portable devices have become an important issue nowadays. Today, environmental monitoring for temperature and CO_2 emissions can be analysed using sensor networks [8]. However, although there was significant progress in energy storage, this improvement was not able to keep up with the dynamic development of microprocessors, electronics, and wireless technologies. To conduct battery maintenance for a large-scale network is very challenging especially when it consists of hundreds to thousands of sensor nodes situated in a limited accessibility place or hazardous environment [9]. In addition, batteries have a short lifespan, and their disposal contributes to environmental issues [10]. Therefore, the conventional power source such as batteries acts as a barrier to the advancement of technologies, Internet of Things (IoT), and Machine to Machine (M2M) communications. Hence, there is a growing need to self-power such devices.

Energy harvesting is the science that collects ambient energy and converts it into a more useful form of energy such as electricity. It is a prominent and key emerging technology that may come as a solution to ensure that the energy provision from the environment and thus extend the lifetime of low power electronics [11]. Energy harvesting using piezoelectric and thermoelectric technologies has recently triggered a significant amount of research interest in the academic community [12, 13, 14]. Most of the work, however, does not make use of the potential ambient energy being wasted on highways using both piezoelectric and thermoelectric technologies [12]. To the best knowledge of the author, there are no published studies about the integration of multiple energy harvesting technologies on highways in Malaysia. Therefore, this study presents a design of an energy harvesting system using piezoelectric and thermoelectric technologies, adapted to the environment in Malaysia. To shed light on its feasibility, an experimental model was built and tested to evaluate its performance.

Working Principles of Thermoelectric and Piezoelectric

In 1821, Thomas Seebeck discovered the thermoelectric effect, which directly converted a temperature difference (temperature gradient) to electricity. This phenomenon is also known as the Seebeck effect and takes place due to the thermal diffusion which starts the motion of charge carriers across the temperature gradient in the conductor. The device used for power generation is known as the thermoelectric generator (TEG) module, as shown in figure 1 [8]. The latter consists of several P-type and N-type semiconductors which are connected thermally in parallel but electrically in series. Besides, the system consists of two distinct connectors, where one of the junctions is at a hot temperature T_h, due to a hot source and the other one is at a cold temperature T_c ($T_c < T_h$), due to a heat sink or cold source. These two connectors are of dissimilar metals or semiconductors. A TEG module is very robust, due to the absence of moving components, and thus makes it favourable for high reliable energy harvesting system [15, 16].

The Seebeck effect is defined by equation (1). It is the ratio of the voltage value V, to the temperature difference ΔT or $(T_h - T_c)$. Hence, the higher the temperature gradient, the higher the electricity generated. The dimensionless figure of merit ZT describes the quality of a thermoelectric material. ZT is defined by equation (2), where K refers to the thermal conductivity and ρ is the electrical resistance [17].

$$V = \alpha(T_h - T_c) \tag{1}$$

$$ZT = \frac{\alpha 2}{K\rho}T \tag{2}$$

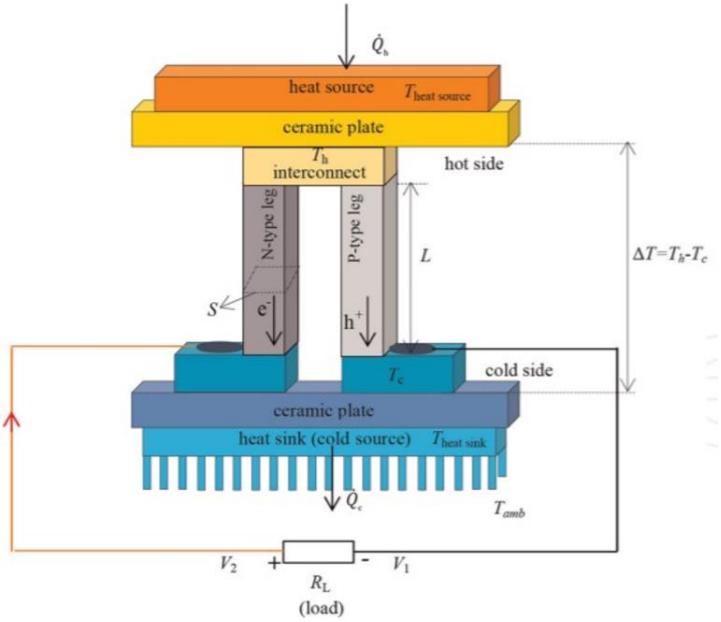

Figure 1. Schematic diagram of TEG [8].

In 1880, the French brothers Pierre Curie and Jacques Curie were the first to experimentally demonstrate the piezoelectric effect. The direct piezoelectric effect is the generation of electricity due to an applied mechanical strain or stress while the reverse piezoelectric effect is the process of generating a mechanical strain by an applied electrical load, using piezoelectric materials [18]. The latter has a crystalline structure without the centre of geometry. When the crystalline structure is deformed (squeezed or stretched) due to applied stress, an electric dipole (known as piezoelectricity) is generated [19]. As the mechanical stress applied to the crystal lattice causes an induce in polarization and an electric field is established across the piezoelectric crystal. There are different types of piezoelectric transducers, however, this study made use of Lead Zirconate titanate (PZT) bimorph circular diaphragm, as shown in figure 2, due to its availability and desirable characteristics of which makes it suitable for energy harvesting on highways [20].

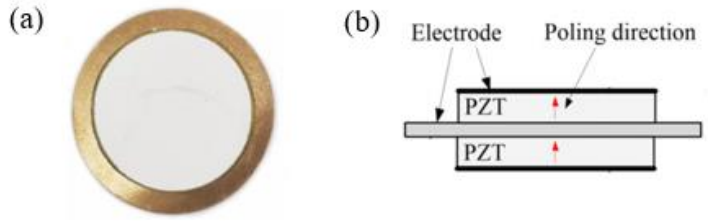

Figure 2. Bimorph piezoelectric circular diaphragm transducer
(a) Front view (b) Side view internal structure [20].

2. Methodology

2.1 Concept and Design of Thermoelectric Energy Harvesting System

The thermoelectric energy harvesting system involves two main systems which are the hot source and cold source. The main objective of these two main systems is to provide a temperature difference to achieve the Seebeck effect, with thermoelectric modules. Since the temperature gradient ΔT or $(T_h - T_c)$ is proportional to the electricity generated V [15]. The thermoelectric energy harvesting model was made using SOLIDWORKS 2018, as shown in figure 3.

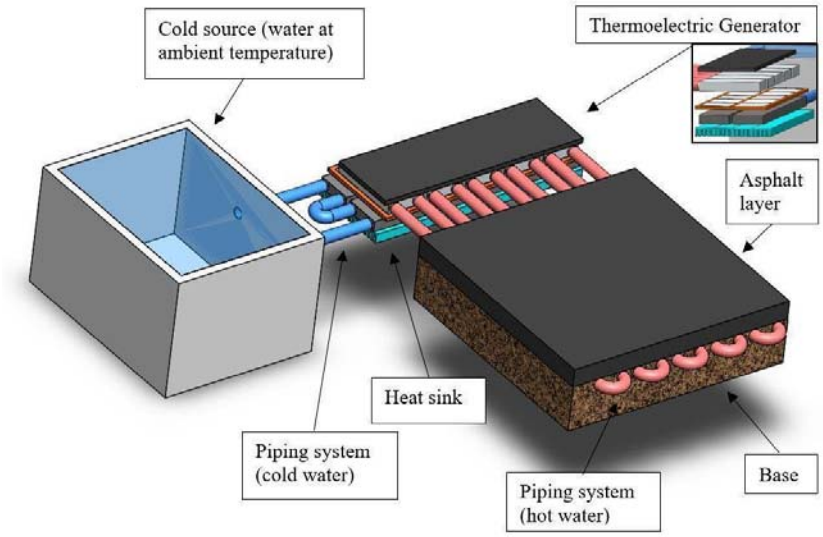

Figure 3. Thermoelectric energy harvesting system layout.

The hot source system aims to collect the ambient thermal energy on the highway and transport it to the hot side of the thermoelectric generator. The targeted thermal energy is the solar radiation and heat release by moving vehicles due to friction and heat dissipated by engines. The method used to transport the thermal energy from the highway to the thermoelectric generator is a pipeline system being embedded in the asphalt layer. Water is used as a working fluid in the pipeline system. This technique was inspired by a method known as pipe-pavement (PP) which is mainly used to reduce the urban heat island effect or to melt snow on the roadway [17]. Asphalt is a good low albedo, absorbs a large amount of heat and thus increases in temperature under hot climate conditions, such as that of Malaysia. The pipelines are embedded at a 2cm depth to catch a large amount of thermal energy [18] and are connected to water heating blocks which are situated on the hot side of the thermoelectric module (the position of the thermoelectric module is shown in figure 4). As hot water in the hot source reaches equilibrium, the hot temperature T_h is achieved.

The objective of the cold source is to achieve the cold temperature T_c at the cold side of the thermoelectric module. The system includes two types of heat sink, a cold-water source, and an aluminium structure heat sink. The cooling blocks are connected by a piping system which used to transfer water from a cold-water source to the cooling blocks and back to the cold-water source. The cold-water source aims to give a relatively constant temperature at all times while dissipating the heat that is conveyed across the thermoelectric generator [7]. In addition, the heat sink is also aerodynamically designed to create a turbulent flow of air, hence increasing the cooling effect. The heat sink is attached to the cold side of the thermoelectric modules. Thus, temperature T_c is achieved.

To ensure a good trade-off between energy conversion efficiency and cost, both material selection and geometry design were taken into consideration. The justification of materials, dimensions, and components are summarized in table 1.

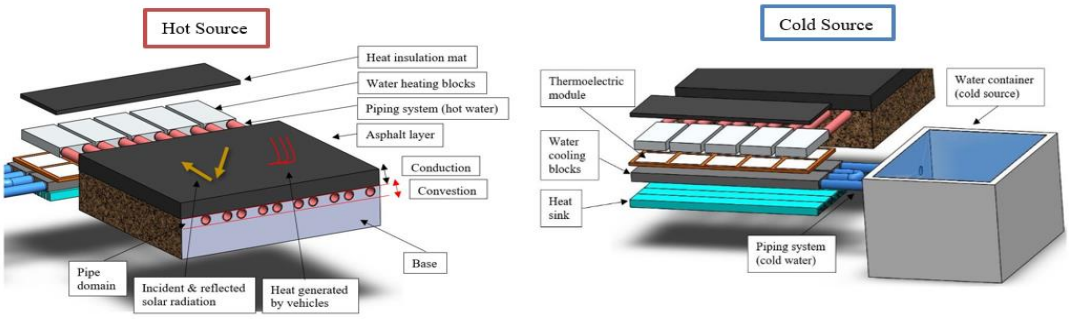

Figure 4. Exploded view of hot and cold source layout.

Table 1. Justification of materials, dimension, and components for thermoelectric EH system.

Item	Specifications	Justifications
Thermoelectric (TE) Module	The thermoelectric module is a Bismuth Telluride ceramic of 40 mm×40 mm and has a Seebeck coefficient of 0.045 V/°C. The system involves 10 TE modules.	This particular thermoelectric module (SP1848-27145) was selected due to its satisfactory thermoelectric ability, relatively cheap cost, and availability. It is specifically designed for power generation. Besides, the operating temperature module (being 0 °C to 150 °C) covers the working temperature range of the energy harvesting system [21]. The number of TE modules used is reasonably acceptable for the budget allocated for this study.
Pipeline	Made up of Aluminium and had a diameter of 10 mm	Due to corrosion resistance and thermal conductivity of 187 W/m.K [15]. The diameter should be within the range of 10 mm. According to Bobes-Jesus *et al* [22], the pipeline depth should be 20 mm from the asphalt surface
Road Model	Consists of two layers, a cold mix asphalt type layer and a base (mixture of sand and soil).	From the resource available for this study, it was fair to use cold mix asphalt which consists of CM-120 cold mix binder, prime coating, chip stones and surrey materials. While the base is a mixture of soil and sand [23].
Water heating blocks	It is made up of aluminium with thermal conductivity of 187 W/m.K [15]. Each having a dimension of 80 mm ×40 mm×12 mm (standard dimension).	To keep the heated water enough and on the total surface area of the hot side of the thermoelectric module. It would help to achieve thermal equilibrium and maintain T_h. It is made up of aluminium due to its good thermal conductivity and has a heat insulation mat on top. The latter would minimize thermal energy dissipation and the black colour surface takes advantage of heat absorption [15].
Water Cooling Block	It is made up of aluminium with thermal	To keep the chilled water enough and on the total surface area of the cold side of the thermoelectric

	conductivity of 187 W/m.K [15]. Each has a dimension of 240 mm ×40 mm×12 mm (standard dimension).	module. It would help to achieve thermal equilibrium and maintain T_c. It is made up of aluminium due to its good thermal conductivity [15].
Cold Source (water tank)	5L cooler jug is partially covered with a lid and placed slightly away from the hot source, to minimize the change in temperature T_c.	In real-life scenarios, the water cold source will be a nearby river or lake, and a self-sustained pump such as a solar-powered pump would be used to initiate the desired flow. However, from the resource available for this study, it was fair to use a 5L cooler jug as it is large enough sufficient to absorb the heat dissipated by the TEG and stay at a constant temperature, due to the relatively bigger volume.

As for the experimental design, statistical data used to model the Malaysian highway was taken as boundary data. Beddu *et al*. [24] reported that the asphalt pavement in Malaysia can reach up to 59.5 °C. According to an experimental study conducted in Malaysia, the water temperature is 24.2 °C [25]. It is fair to assume that the maximum temperature that the hot source can achieve is 60 °C and the cold source is at a temperature T_c of 24 °C. The data of hot source and cold source were rounded off to ease the data collection for the experiment. To heat the asphalt pavement model, a 1000W infrared heating lamp is used. The water cold source is maintained at 24 °C in a 5L covered cooler jug so that the water stays chilled. The experimental setup is shown in figure 5. By using three waterproof temperature sensors (with digital output screen), the temperature hot source (asphalt), T_h and T_c can be monitored. The Seebeck effect is achieved by the temperature difference created by the hot and cold sides of the thermoelectric module. The open-circuit voltage V as well as short circuit current I generated by the system would be measured using two individual multi-meters.

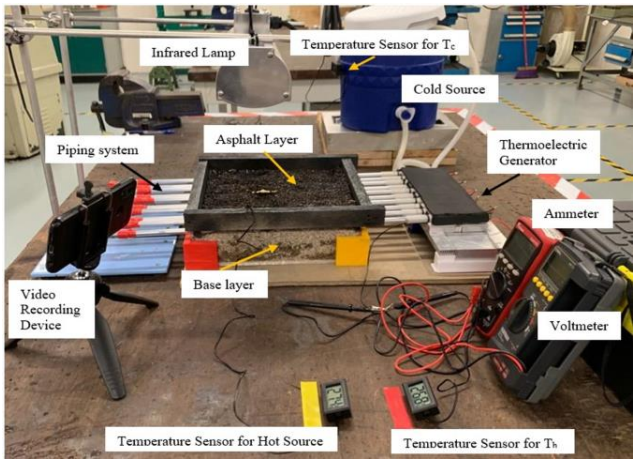

Figure 5. Experimental setup for thermoelectric energy harvesting system.

2.2 Concept and Design of Piezoelectric Energy Harvesting System

The goal of the piezoelectric energy harvesting system is to use the energy from moving vehicles to generate electricity, through the piezoelectric effect. Moving vehicles generate impact, stress, and a range of vibration on the highway which leads to a considerable waste of energy and deformation of the road [5]. The amount

of ambient energy is based on the type of vehicle and speed. This design focuses on converting mechanical stress and slight deformation of the road by one wheel of the vehicle into electricity. The design consists of one piezoelectric layer embedded between two asphalt layers. The sides of the PZT bimorph or piezoelectric transducer are sandwiched between two thin silicon rubber layers, acting as supports. Figure 6 illustrates the piezoelectric energy harvesting model and an exploded view of the model.

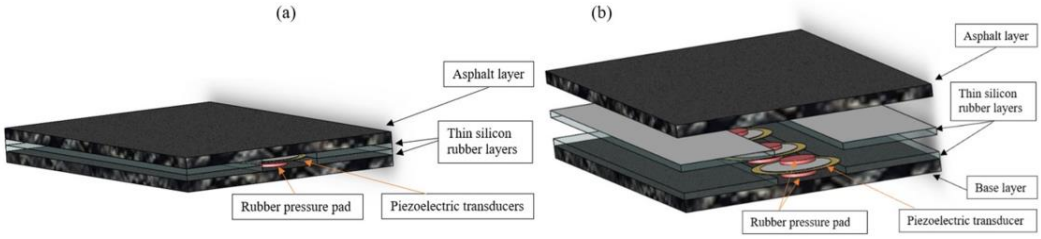

Figure 6. (a) Piezoelectric energy harvesting model, (b) Exploded view of the model.

Rubber pressure pads are used to apply stress on the piezoelectric transducers when the road experiences stress, as shown in figure 7. As soon as the model is loaded, the piezoelectric experiences deformation and the maximum deflection of the road model is approximately 2 mm. The latter would help to protect the piezoelectric transducers and ensure that the system does not affect the performance of the road.

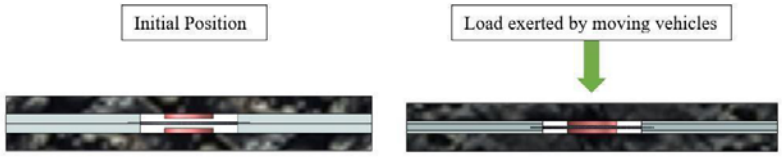

Figure 7. Initial and final position of piezoelectric model.

The justification of materials, dimensions and components are summarized in table 2.

Table 2. Justification of materials, dimension and components for piezoelectric EH system.

Item	Specifications	Justifications
Piezoelectric Transducer	PZT bimorph circular diaphragm type of transducer. It is made up of lead zirconate titanate (PZT) [20]. 3 Transducers are connected in series. Diameter of 50 mm.	This transducer was selected due to the limited choice available on the market and its affordable cost. Also, it has desirable characteristics which makes it suitable for harvesting energy from mechanical stress and deformation [20]. The piezoelectric is capable of generating more power when connected in series [26].
Thin Silicon Rubber Layer & Pressure Pad	Two layers of 4 mm thickness each. The surface area of the rubber pressure pad is 700 mm^2.	Rubber is used compared to another hard material, as it would not permanently damage the piezoelectric during high impact. The layers help to support the piezoelectric transducer and protect the device from having direct contact with the asphalt aggregate [20]. The surface area is large enough to not exceed the

		yield strength of the piezoelectric materials, which is 250 MPa, which thus is not exceeded [27].
AC-DC Converter	Full-wave bridge rectifier.	A piezoelectric transducer gives AC voltage and thus an AC-DC convertor is required to bring the voltage to DC [10].

Moving on to the experimental design, loads are applied to simulate the stress exerted by moving vehicles on highways. The experimental setup is illustrated in figure 8. In this study, the contact stress exerted by one wheel of the vehicle on the piezoelectric model is investigated, assuming equal weight distribution on the four wheels. The range of loads used in the experiment can cover the normal stress which the quarter weight of the compact car (910 kg), midsized car (1540 kg) and truck size (1710 kg) would exert on the road [28]. Since, normal stress is defined as axial force applied per cross-sectional area [29], even if the loads used in this experiment are way smaller, the stress would be as high as the real-life scenario. As the cross-sectional area of the loads used in this experiment is much smaller in contrast to the contact patch area for the wheel of a vehicle. Assume the average contact patch area of a vehicle tyre is 17950 mm^2 [24]. The stress caused by one tyre of the compact car, midsize car and truck size are summarised in table 3. The resulting stress by the loads used in the experiment is summarised in table 4. Eleven different loads were used to obtain a range of data to plot the desirable graphs and higher loads than 110 N could not be used due to the limited resources available for this study.

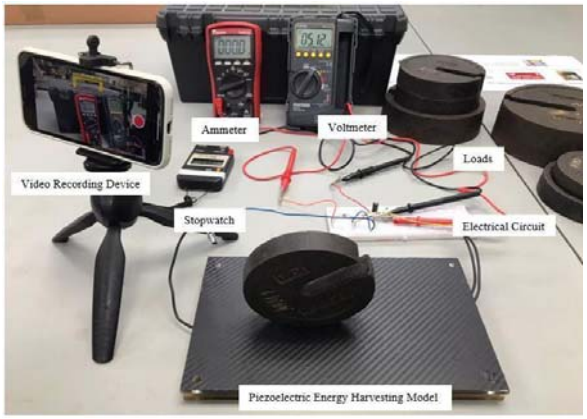

Figure 8. Experimental setup for piezoelectric energy harvesting system.

Firstly, the vertical deformations were measured using a Vernier calliper. Secondly, the peak Ac voltage was measured. Thirdly, the piezoelectric system was connected to the full-wave rectifier circuit and the open circuit DC voltage was measured. Lastly, a capacitor was introduced in the circuit to temporarily store the energy, the current, the voltage across the capacitor, charging and discharging time of the capacitor, were measured, respectively. All the experiments were repeated three times for each load used and averaging was done to minimize random errors. The experiment was video recorded to help the experimenter accurately collect desired data at any instant during playback of the video in slow-motion. The output power P can be calculated using equation (3) [30].

$$P = I \times V \tag{3}$$

Table 3. Summary of reference data for compact car, midsize car and truck size vehicle.

Types of Vehicles	Weight, W (kg) [28]	Quarter Weight, (9.81W/4) (N)	Average Contact Patch Area, A_p (mm^2) [31]	Stress of one wheel on the road (9.81W/4)/Ap (kPa)
Compact Car	910	2231.78	17950	124.33
Midsize Car	1540	3776.85	17950	210.41
Truck size	1710	4193.775	17950	233.64

Table 4. Loads and corresponding stress.

Loads (N)	10	20	30	40	50	60	70	80	90	100	110
S, Area (mm^2)	96	168	216	280	344	352	396	405	414	450	468
Stress (kPa)	104.17	119.05	138.88	142.86	145.35	170.45	176.76	197.53	217.39	222.22	235.04

3. Results and Discussion

3.1 Thermoelectric Energy Harvesting System

The first step in evaluating the thermoelectric energy harvesting model, as shown in figure 5, focused on measuring the open-circuit output voltage as well as current generated when the hot source is heated from 30 °C to 60 °C. For every 3 °C increments the latter, the temperature of the hot side of the thermoelectric module, T_h, open-circuit voltage V and current, I was recorded. While the cold side of the thermoelectric, T_c was maintained at 24 °C by using chilled water from a 5L covered cooler jug. The experiment was repeated 4 times and averaging was done to mitigate human errors. Figure 9 displays the experimental data of voltage V generated for various temperature differences ΔT. Besides, the theoretical data of output voltage for these temperature differences were calculated using equation (1) and plotted on the same graph.

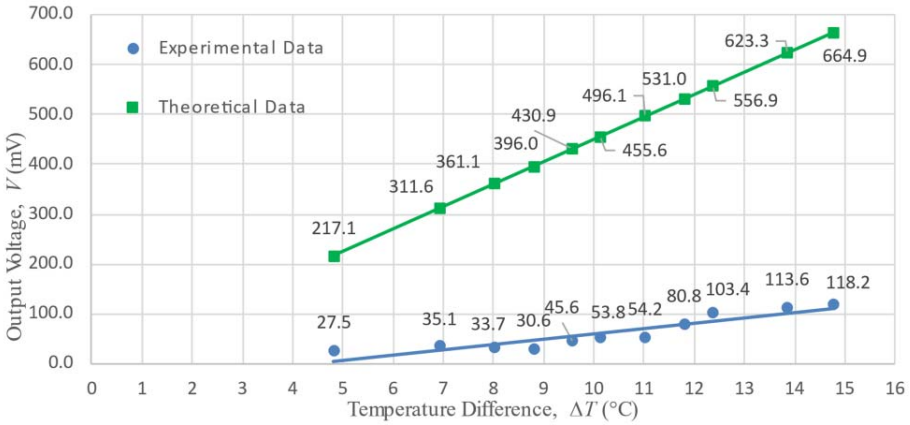

Figure 9. Open circuit voltage (mV) for various temperature difference (°C).

Based on figure 9, the theoretical data indicate a linear relationship between the output voltage and temperature difference, where the gradient is constant and represents the theoretical Seebeck coefficient α (0.045 V/°C). The theoretical data express the maximum voltage the thermoelectric energy harvesting system can achieve for that temperature difference. The output voltage increases with the increase of temperature difference, which agrees with the Seebeck effect. The line of best fit for the experimental results shows the same trend. However, the output voltages in the experimental data are noticeably lower than the theoretical one. This can be explained by the lower Seebeck coefficient that the thermoelectric achieved

during the experiment; the experimental data line is less steep and thus, the Seebeck coefficient was found to be 0.010673 V/°C (gradient of line). The highest output voltage recorded during this experiment was 118.2 mV at a temperature difference of 14.8 °C. In practice, the sides of the thermoelectric modules do not achieve T_h and T_c uniformly throughout their surface area, due to material surface imperfections and heat dissipation. In addition, the modules work at different temperatures simultaneously, as the infrared lamp does not heat the asphalt model uniformly and thus, each module generates a different electromotive force [32]. This justifies the lower output voltage in the experimental data.

To evaluate the output power P the thermoelectric system can deliver for the same temperature difference as in figure 9, the open-circuit voltage V and current, I recorded, were used to calculate the output power P, using equation (3). Figure 10 shows the output power P for the various temperature differences.

According to figure 10, output power increases with the increase of temperature difference. The highest output power is 1.06 mW at a temperature difference of 14.8 °C. Therefore, the hot source is heated up to 60 °C while the cold source is at a temperature of 24 °C, the thermoelectric energy harvesting system can generate 1.06 mW.

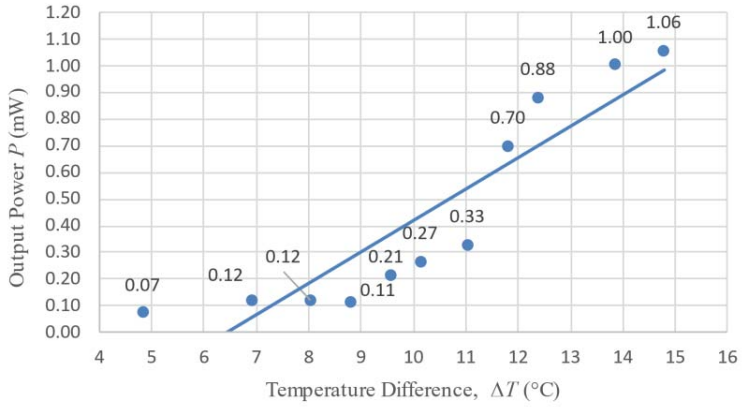

Figure 10. Output power (mW) for various temperature difference (°C).

In the above scenario, the electrical characteristics of the thermoelectric energy harvesting system were evaluated when the temperature gradient increases from 30 °C to 60 °C, and the responses were investigated. However, in real-life scenario, the hot source is exposed to sunlight for a long period of time, which in this study was taken as 6h, the mean daily sunlight in Malaysia [24]. Hence it was also important to investigate the response of the system when the hot source is exposed to sunlight for a long period of time. Figure 11 illustrates a multiple bar chart of the open-circuit voltage and the output power for every 1h interval.

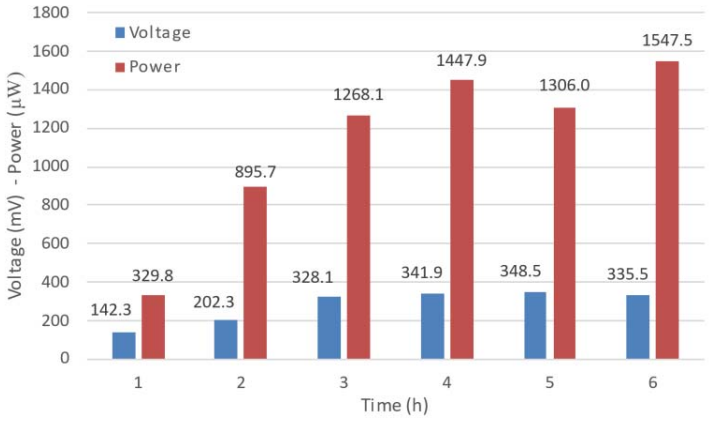

Figure 11. Multiple bar chart of Voltage (mV)- Power (μW) vs. Time (s).

According to the chart in figure 11, there were upward trends in both the voltage and the power, during the first 4 hours. During the last 2 hours the rise in voltage and power became less significant. The maximum power acquired after 6 hours and found to be 1547.5 μW or 1.55 mW. However, the maximum voltage recorded was 348.5 mV, which was obtained after 5 hours.

The trend of the output power yield as well as open-circuit voltage is related to the temperature difference. As the latter rises from 11.7 °C to 17.2 °C during the first 4 hours, which explains the noticeable increase in power and voltage yield. Since according to the Seebeck effect, the voltage acquired is directly proportional to temperature gradient [15]. On the other hand, there were no significant change in the temperature difference, which indicates that the system has reached thermal equilibrium after 4 hours. Therefore, the thermoelectric energy harvesting system reaches its thermal stabilization over time and the maximum output power limit is achieved. Besides, considering the thermal behaviour, according to the first law of thermodynamics the energy input, which in this case is the heat source, can never exceed or be equal to the energy output, which is the hot side of the thermoelectric [24]. For instance, while the hot source (asphalt) is being heated at 60 °C, the highest temperature achieved at the hot side of the thermoelectric T_c, was 41.2 °C, meaning that the maximum heat transfer efficiency is approximately 31.3%. The slight drop in power and voltage during the 5- and 6-hours period, respectively, can be viewed as a small performance deterioration of the TEG over long operating hours. Memon and Tahir [33] confirmed a slight deterioration in the performance of the same TEG in terms of short-circuit current and open-circuit voltage, while the temperature gradient was kept constant, during their second test.

3.2 Piezoelectric Energy Harvesting System

The total displacement in terms of vertical deformation of the piezoelectric model, for each applied load, was first evaluated. For each load applied to the model, the vertical deformations were measured at three different locations and the average vertical deformation was calculated. Figure 12 shows the average vertical deformation for each load.

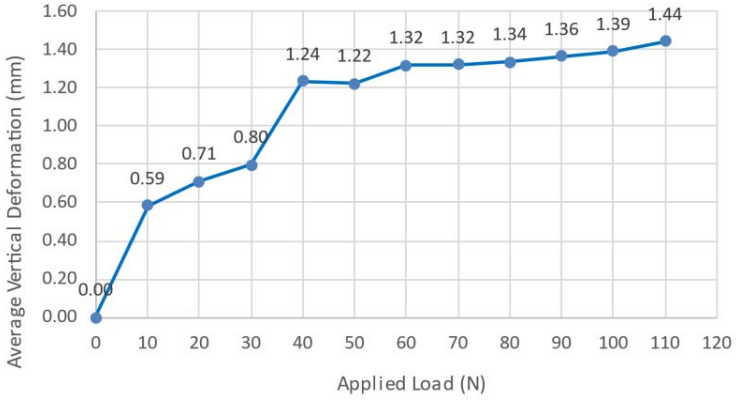

Figure 12. Average vertical deformation (mm) under various loads (N).

Figure 12 shows that as the applied load increases, the vertical deformation/displacement of the piezoelectric model also increases, reaching a maximum vertical deformation of 1.44 mm under the 110 N load. The percentage difference in the vertical deformation decreases as the load increases, as the slope of the graph gradually decreases. The percentage increment in the vertical deformation between, 10 N and 20 N is 20.3% while for 100 N and 110 N, it is 3.6%. This is because as the load increases the normal stress encountered by the piezoelectric model also increases, as calculated in table 4. The latter causes the piezoelectric model to experience compression due to the elastomer property of the thin silicon rubber layers and rubber pressure pad. Thus, the aim of having a maximum deformation of less than 2 mm, so that the performance of the road to not be affected, is achieved. However, the vertical deformation decreases as the elastic modulus of the thin silicon rubber layers and rubber pressure pad are non-linear [34]. Hence, the piezoelectric transducer experiences deformation, assuming a linear relationship with the piezoelectric model. By right, the piezoelectric effect is achieved, and an electric voltage is generated [19], as shown in figure 13.

The second step in evaluating the piezoelectric energy harvesting system was to measure the peak alternating current (AC) voltage for each load applied, as illustrated in figure 13. The polarity of the voltage was not taken into consideration as the objective in this step was to record the instantaneous peak voltage which the system can achieve due to various loads.

Figure 13 shows clearly that the Peak AC voltage rises as the applied load increases. The percentage increment of the peak AC voltage decreases as the load increases, as the graph becomes less steep. The percentage increment of the peak AC voltage between 10 N and 20 N is 51.7% while for 100 N and 110 N, it is 6.6 %. This rise in AC voltage can be explained by the fact that, as the applied load increases, the stress experienced by the piezoelectric model increases and therefore the deformation encountered by the piezoelectric transducer also increases, as proven by figure 12. Therefore, according to the direct piezoelectric effect, as the deformation of the piezoelectric material increases, the generated electric field also rises [30]. Although the strain experienced by the piezoelectric material has a linear relationship with the generated voltage, it is however not the case in figure 13, as the vertical deformation is not linear to the applied load.

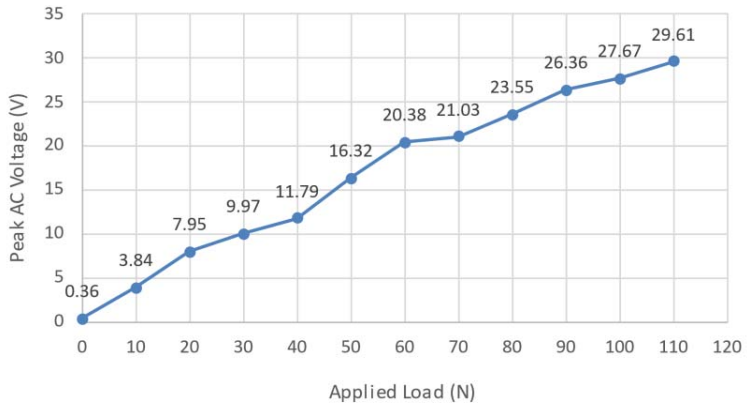

Figure 13. Peak AC voltage (V) under various loads (N).

Since AC voltage cannot be stored and it is more appropriate to power digital devices with DC voltage, the AC voltage produced by the piezoelectric transducers had to be converted to DC voltage. A full-wave bridge rectifier circuit is used [30]. Figure 14 displays the relationship of peak DC voltage for various applied loads. This peak DC voltage is the open-circuit voltage measured using a multi-meter.
According to figure 14, the rise is significant in the early stage of the graph, from 0 N to 40 N, and gradually becomes gentle in the later stage, from 50 N to 110 N. The maximum voltage recorded was 9.83 V, under an applied load of 110 N. The experimental results displayed in figure 14, supports the findings in figure 12, as the percentage increment of vertical displacement decreases, so does the peak DC voltage. However, a significant peak voltage drop is observed as the AC voltage is converted to DC voltage, 19.78 V voltage drop in the maximum peak voltage. The use of cheap diodes in the bridge rectifier, extensions and joining of wires which increases resistance as well as creates losses in the circuit can explain the noticeable voltage drop. The latter can be viewed as a limitation of this experiment, but the optimization of the electrical circuit is not part of the scope of this study.

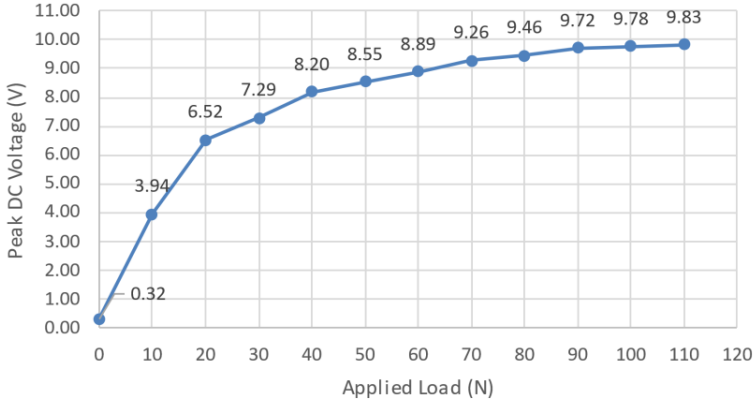

Figure 14. Peak DC voltage (V) under various loads (N).

The peak DC voltage measured in figure 14 is not consistent, as the load is changed or removed, the voltage changes accordingly. Thus, for the last step in evaluating the piezoelectric energy harvesting system, a capacitor is introduced to the circuit. The aim was to show that the system is capable of delivering a

consistent voltage under various loads applied. In this experiment, the load was applied on the piezoelectric model every 3 s, until the capacitor is charged, this cyclic applied load is maintained or dwelled for 10 s and then removed to allow the capacitor to discharge. The reason for having the dwell was to investigate whether the system can maintain the same voltage as long as the cyclic load is maintained. Figure 15 shows the charging, dwell, and discharge time of the system for each load used. The voltage was measured across the capacitor. An ammeter was also connected in series to measure the peak current.

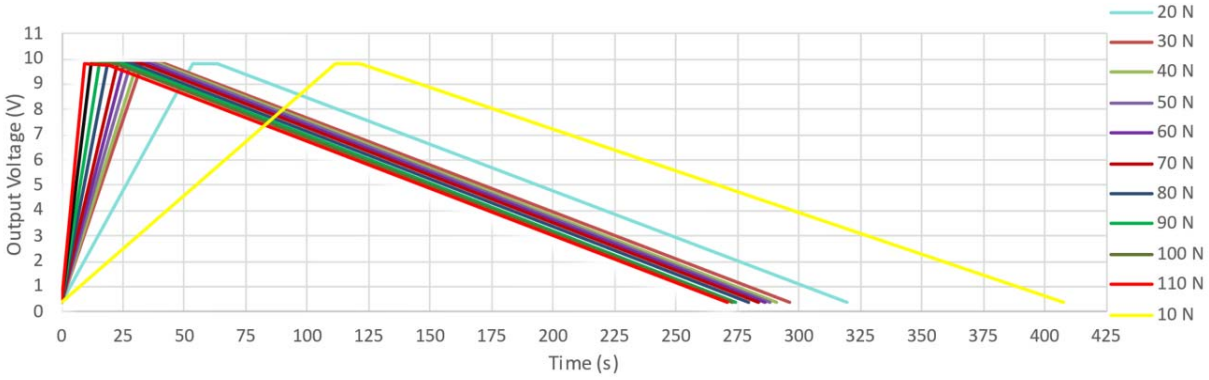

Figure 15. Output voltage (V) against charging, dwell and discharge time (s) for various loads (N).

According to figure 15, all the loads used in this experiment could fully charge the capacitor to a maximum output voltage of approximately 9.8 V. The discharging time of the capacitor is almost the same for each load used, as the average discharging time is 250 s and also, the slope for the discharging portion is the same. In addition, during the dwell time of 10 s, the voltage remains constant, as the line is horizontal for this portion of the graph. The latter seems small as the dwell time used for this experiment was only 10 s, which is small relative to the charging and discharging time. However, as the applied load increases, the graph skewed to the left, the charging segment of the graph becomes steeper. This is because it takes less time to fully charge the capacitor using heavier loads. The latter provides more electric voltage, as shown in figure 14. Hence, this step of the experiment proves that the system can provide a consistent voltage as long as the piezoelectric model experiences mechanical stress. As the capacitor smoothen the output voltage [35] Larger normal stress causes more deformation to the piezoelectric transducer which results in more mechanical energy being converted to electricity. It takes a significant time for the system to be discharged as compared to the charging time. The average maximum current I recorded was 20.8 μA. When the capacitor is fully charged, the output voltage V is 9.80 V. Thus, using the mathematical correlation in equation (3), the output power of the system was calculated and found to be 0.2 mW. Therefore, one wheel of a moving vehicle on the highway would produce 0.2 mW using the piezoelectric energy harvesting system.

4. Large Scale feasibility assessment

The experimental results for the thermoelectric energy harvesting system prototype shows evidence that a heat collector area of 0.25 m × 0.25 m could generate a maximum average power output of 1.55 mW over a period of 6h per day. While the piezoelectric energy harvesting unit gave evidence that a single wheel of the vehicle could generate a maximum average output power of 0.2 mW. The prototypes proposed in this study was validated based on experimental testing using parameters which represent actual conditions. Hence, the prototypes could be conidered as an individual harvesting unit to estimate the capability of the large-scale implementation in real-life. Table 5 summarize the large scale performance estimation.

Table 5. Summary of large scale performance estimation.

	Thermoelectric	**Piezoelectric**
Large scale size	4 lanes of 1km length and 3.75 width.	Two rows in 1 lane of 1 km length, with 10 m longitudinal spacing.
Power per square meter (mW/m^2)	24.8	5.33
Energy in watt-hour (Wh)	2230	0.384
Energy in Joules (J)	8.04×10^6	1.35×10^3
Power Density (mW/cm^3)	0.028	0.023

5. Conclusion

This study focuses on converting the waste thermal and mechanical energy available on the highway, into electricity. This electricity can be used for other activities such as to support low-power electronics. A design for thermoelectric and piezoelectric energy harvesting system, adapted to Malaysian highway conditions, was presented. Both systems were built and experimentally tested. From the results obtained, it can be deduced that the implementation of both piezoelectric and thermoelectric, as energy harvesting devices on highways, have potential utility as green micro-power generation. However, this system might not yet be economically benefit. The findings for this study are summarized as follows.

Thermoelectric energy harvesting system:

- Under Malaysian highway conditions, the system reached thermal equilibrium after 4h and a maximum temperature difference of 17.2 °C was recoded, at a maximum heat transfer efficiency is approximately 31.3%. The thermoelectric energy harvesting system could achieve a maximum, open-circuit voltage of 348.5 mV and output power of 1.55 mW.
- The energy produced on a large scale was estimated to be 2.23 kWh, which was equivalent to 24.8 mW/m^2.
- Its levelized cost of energy was at 0.50 RM/kWh.

Piezoelectric energy harvesting system:

- A peak AC voltage of 29.61 V was recorded for a maximum vertical deformation of 1.44 mm, under the 110N. The latter caused a normal stress of 235.04 kPa on the piezoelectric model.
- The peak AC voltage was converted to DC voltage using a full-wave bridge rectifier. The maximum peak DC voltage recorded was 9.83 V, under 110 N. However, a significant voltage drop was observed in the conversion of AC to DC voltage which can be viewed as limitation.
- To overcome the limitation of inconsistent voltage, a capacitor was added to the electrical circuit. By charging, having a dwell time and allowing the capacitor to discharge, under the various loads used, the results proved that the piezoelectric system could provide a consistent output voltage as long as the system experienced normal stress. The system could produce an output power of 0.2 mW.
- The energy produced on a large scale was estimated to be 0.384 Wh, which was equivalent to 5.33 mW/m^2.
- Its levelized cost of energy was 0.62 RM/kWh.

Moving on to the future goals for this study, both thermoelectric and piezoelectric system could be combined through the hybrid method and tested experimentally. Then, the large-scale implementation could be justified in terms of performance and its economic benefits. The authors suggest future research to focus on the on-field testing to evaluate the performance in real-life conditions and to work toward optimizing the AC to DC voltage conversion as well as improving the temperature gradient by minimizing thermal losses.

It is highly recommended to implement micro energy harvesting in the Feed in Tariff (FiT) Malaysia. As it will encourage companies and universities to conduct future research towards developing this emerging field.

Acknowledgements
The authors would like to extend their sincere thanks to Taylor's University and the School of Engineering staff for providing guidance, and to all the lab assistants that contributed to the betterment of this project by offering their facilities to be utilized in the best way.

References
[1] Han F, Bandarkar A W and Sozer Y 2019 Energy harvesting from moving vehicles on highways *Proc. 2019 IEEE Energy Conversion Congress (ECCE).* Baltimore, MD, USA, pp 974-978
[2] Energy Commission 2018 *Malaysia energy statistics handbook* (Suruhanjaya Tenaga (Energy Commission)) pp 1-86
[3] Zoui M A, Bentouba S, Stocholm J G and Bourouis M 2020 A review on thermoelectric generators: Progress and applications *Energies* **13(14)** p 3606
[4] Zhang Z, Xiang H and Shi Z 2016 Modeling on piezoelectric energy harvesting from pavements under traffic loads *J. Intell. Mater. Syst. Struct.* **27(4)** pp 567-578
[5] Xu X, Cao D, Yang H and He M 2018 Application of piezoelectric transducer in energy harvesting in pavement *Int. J. Pavement Res. Technol.* **11(4)** pp 388-395
[6] Zabihi N and Saafi M 2020 Recent developments in the energy harvesting systems from road infrastructures *Sustain*. **12(17)** 6738
[7] Jiang W *et al* 2017 Energy harvesting from asphalt pavement using thermoelectric technology *Appl. Energy* **205** pp 941-950
[8] Thakare P and Ambudkar B 2017 Study and analysis of CO_2 emission control methods for wireless networks *Proc. 2017 2nd Int. Conf. on Communication and Electronics Systems* (*ICCES*) pp 742-745
[9] Yildiz F 2009 Potential ambient energy-harvesting sources and techniques *J. Technol. Stud.* vol. **35(1)** pp 40-48
[10] Nozariasbmarz A *et al* 2020 Review of wearable thermoelectric energy harvesting: From body temperature to electronic systems *Appl. Energy* **258** p 114069
[11] Shaharizal, S, Ahmad, M R and Hawari, H F 2017 Design and analysis of a hybrid energy harvester for self-powered sensor *IEEE Reg. 10 Annu. Int. Conf. Proceedings/TENCON*, pp 1016-1021
[12] Guo L and Lu Q 2017 Potentials of piezoelectric and thermoelectric technologies for harvesting energy from pavements *Renew. Sustain. Energy Rev.* **72** pp 761-773
[13] Thein C K, Ooi, B L and Liu, J S 2016 Modelling And optimisation of a bimorph piezoelectric cantilever beam in an energy harvesting application *J. Eng. Sci. Technol*. **11(2)** pp 212-227
[14] Salah W A and Abuhelwa M 2018 Review of thermoelectric cooling devices recent applications *J. Eng. Sci. Technol.* **15(1)** pp 455-476
[15] Khamil, K N, Mohd Sabri, M F and Yusop, A M 2020 Thermoelectric energy harvesting system (TEHs) at asphalt pavement with a subterranean cooling method *Energy Sources, Part A Recover. Util. Environ. Eff.* **00** pp 1-17
[16] Abdal-Kadhim A M and Leong K S 2018 Application of thermal energy harvesting in powering WSN node with event-priority-driven dissemination algorithm for IOT applications *J. Eng. Sci. Technol.* **13(8)** pp 2569-2586
[17] Zhu X, Yu Y and Li F 2019 A review on thermoelectric energy harvesting from asphalt pavement: Configuration, performance and future *Constr. Build. Mater.* **228** p 116818.
[18] Sun W *et al* 2018 The state of the art: application of green technology in sustainable pavement *Adv.*

Mater. Sci. Eng. **2018** Article ID 9760464
[19] Pohanka M 2017 The piezoelectric biosensors: Principles and applications, a review *Int. J. Electrochem. Sci.* **12** pp 496-506
[20] Chen Y *et al* 2016 Mechanical energy harvesting from road pavements under vehicular load using embedded piezoelectric elements *J. Appl. Mech.* **83(8)** pp 1-7
[21] Li S *et al* 2017 The thermoelectric analysis of different heat flux conduction materials for power generation board *Energies* **10(11)** 1781
[22] Bobes-Jesus V *et al* 2013 Asphalt solar collectors: A literature review *Appl. Energy* **102** pp 962-970
[23] García A and Partl M N How to transform an asphalt concrete pavement into a solar turbine *Appl. Energy* **119** pp 431-437
[24] Beddu *et al* S 2018 Thermal behavior of asphalt pavement as an active solar collector under Malaysia climate condition using rubber tube *J. Eng. Appl. Sci.* **13(7)** pp 1690-1695
[25] Ahmad M H *et al* 2013 The effect of air temperature on water temperature via traditional and statistical experimental design in Johor Bahru (Malaysia) *IOSR J. Appl. Geol. Geophys.* **1(1)**, pp 49-52.
[26] Jha B K and Ray M C 2019 Benchmark analysis of piezoelectric bimorph energy harvesters composed of laminated composite beam substrates *Int. J. Mech. Mater. Des.* **15** pp 739-755
[27] Mo C, Radziemski, L J and Clark W 2010 Analysis of piezoelectric circular diaphragm energy harvesters for use in a pressure fluctuating system *Smart Mater. Struct.* **19**, 025016
[28] Shin Y H *et al* 2018 Piezoelectric polymer-based roadway energy harvesting via displacement amplification module *Appl. Energy* **216** pp 741-750
[29] de Cagny H *et al* 2019 The yield normal stress *J. Rheol.* **63(2)** 285
[30] Covaci C and Gontean A 2020 Piezoelectric energy harvesting solutions: A review *Sens.* **20(12)** 3512
[31] Krmela J, Beneš, L and Krmelová, V 2012 Statical experiments of tire as complex long-fibre composite for obtaining material parameters and deformation characteristics *Mater. Eng.* **19** pp 124-135
[32] Wang Y T, Liu, W, Fan, A W and Li P 2013 Performance comparison between series-connected and parallel-connected thermoelectric generator systems *Appl. Mech. Mater.* **327** pp 327-331
[33] Memon S and Tahir K N 2018 Experimental and analytical simulation analyses on the electrical performanceof thermoelectric generator modules for direct and concentrated quartz-halogen heat harvesting *Energies* **11(12)** p 3315
[34] Butler T I 2018 *Blown Film Processing Handbook of Industrial Polyethylene and Technology: Definitive Guide to Manufacturing, Properties, Processing, Applications and Markets* ed M A Spalding and A M Chatterjee (Scrivener Publishing LLC) Chapter 12 pp 381-410
[35] Abdal M A and Leong K S 2017 Piezoelectric pre-stressed bending mechanism for impact-driven energy Harvester *IOP Conf. Ser.: Mater. Sci. Eng.* **210** 012307